ChemComm

Accepted Manuscript

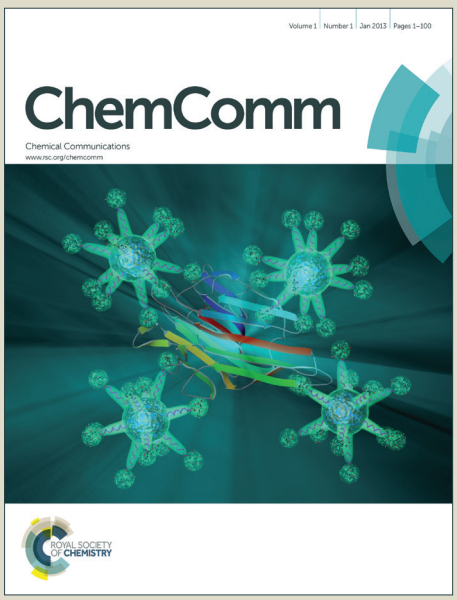

ROYAL SOCIETY OF CHEMISTRY

www.rsc.org/chemcomm

Journal Name

COMMUNICATION

Synthesis of well dispersed polymer grafted metal-organic framework nanoparticles

Received 00th January 20xx,
Accepted 00th January 20xx

DOI: 10.1039/x0xx00000x

www.rsc.org/

K. Xie [a], Q. Fu [a], Y. He [a], J. Kim [a], S. J. Goh [a], E. Nam[a], G. G. Qiao*[a], P. A. Webley*[a]

Novel polymer grafted metal-organic framework (MOF) nanoparticles were synthesized. The formed core/shell nanoparticles exibit outstanding water dispersity and pH sensitivity, and show their catalytic effect for the reduction reaction of 4-nitrophenol (NP) to 4-aminophenol (AP) when loaded with Pd(0) catalyst.

Metal-organic frameworks (MOFs) are porous materials consisting of metal ions and organic ligands.[1] Due to the tunability of the pore structure and functional groups,[2,3] MOFs have been used in a wide range of fields including small molecule adsorption/separation, catalysis, electronic/optic/sensing devices and biomolecule/drug delivery.[4–7] When applying MOFs in aqueous environments, the strong aggregation tendency of MOF particles hampers their performance by increasing mass transfer resistance, reducing interfacial area and enlarging particle size. The modification on MOF particles with polymer could be an efficient way to supress their aggregation tendency. However, the previous works on MOF/polymer composites mainly focus on their enhanced biocompatibility and water stability, yet the improvement on MOF particle aqueous dispersity in MOF/polymer composite particles has not been reported.[7–11] Indeed, there is still a research gap in the literature concerning 100% dispersion of MOF nanoparticles in water.

In this work, we are aiming to develop novel 100% water dispersible MOF/polymer core-shell composite nanoparticles (P@MOF) via a "grafting-from" approach using an activator regenerated by electron transfer-atom transfer radical polymerization (ARGET-ATRP) technique. This technique has been demonstrated to be a robust radical polymerization technology to initiate formation of a polymer "brush" from solid substrates including 2D surface or 3D particles.[12,13] The polymer effectively improved the dispersity of MOF nanoparticles in water, which, to the best of our knowledge, is the first example of MOF based nanoparticles that 100% dispersed in water. The formed P@MOF nanoparticles were then used as a catalyst carrier to demonstrate the benefit of high dispersity on catalytic activity.

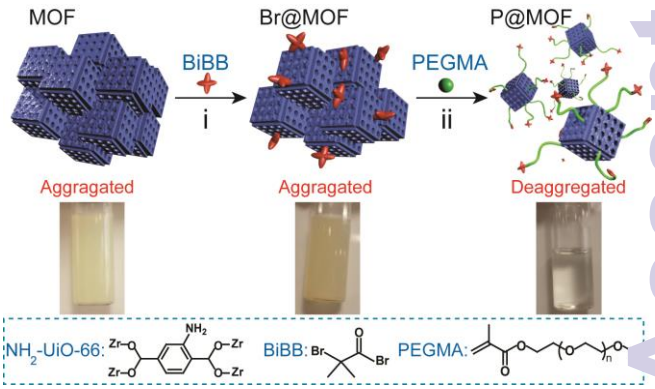

Scheme 1 Schematic representation of the preparation of P@MOF: i) esterification reaction between BiBB and NH_2-UiO-66 using TEA to neutralize HBr and ii) ARGET-ATRP of PEGMA in the presence of $CuBr_2$/Me_6TREN/N ascorbate. Digital photographs reflect the aqueous dispersion of NH_2-UiO-6 (left), 0.5Br (middle) and 0.5Br-4P (right) with the normalized MO concentration of 0.5 mg mL^{-1} at pH=7.

The P@MOF, consisting of a water stable MOF core (NH_2-UiO-66) and a PEG-based shell, was prepared *via* a two-step process as displayed in Scheme 1. Of the many polymers, PEG is perhaps the most ideal, as it is inert, biologically compatible, and soluble in both hydrophilic (*e.g.* water) and hydrophobic (*e.g.* dichloromethane) solvents.[7,10] Firstly NH_2-UiO-66 was functionalized with bromoisobutyryl bromide (BiBB) to obtain the bromo-functionalized UiO-66 (Br@MOF) for the subsequent ARGET-ATRP, and are named xBr, where x denotes the mole feeding ratio of the BiBB to the amine groups (step i). The Br@MOF was then used as a multi-functionalized initiator for the ATRP of a macromonomer poly(ethylene glycol) methyl ether methacrylate (PEGMA) (

[a] *Department of Chemical and Biomolecular Engineering, The University of Melbourne, Parkville, VIC, 3010, Australia. E-mail: gregghq@unimelb.edu.au, paul.webley@unimelb.edu.au*

† Electronic Supplementary Information (ESI) available: [details of experiments and characterization on the composite nanoparticles]. See DOI: 10.1039/x0xx00000x

aqueous solution at ambient conditions (step ii). The resulted P@MOFs are named xBr-yP where y denotes the weight feeding ratio of the PEGMA *vs.* the Br@MOF.

The morphology of NH_2-UiO-66, Br@MOF and P@MOF were characterized by SEM, as shown in Figure 1a-c. It is observed that NH_2-UiO-66 exhibits a spherical morphology with domains in a diameter of 20-70 nm. The particles are highly aggregated and cannot be dispersed by sonification, as shown in Figure 1a, agreeing with the previous report.[14] The digital photograph and dynamic light scattering (DLS) result for NH_2-UiO-66 aqueous suspensions are displayed in Scheme 1 and Figure S1a. As seen, the NH_2-UiO-66 suspension is cloudy due to the aggregation of the particles. The average hydrodynamic diameter (*D*) of NH_2-UiO-66 aggregates in aqueous solution measured by DLS is *ca.* 6 μm. The particle size and aggregation tendency of the Br@MOF is almost identical to the raw NH_2-UIO-66, as suggested by the SEM image (Figure 1b), digital photograph (Scheme 1) and DLS measurements (*D*~4 μm, Figure S1a). After ARGET-ATRP of PEGMA, a spherical morphology with diameter of 20-70 nm for the P@MOF (0.5Br-4P) particles is clearly observed by SEM (Figure 1c). As expected, the aggregation nature of the MOF particles has been dispersed by our polymer modification, as observed from morphology in SEM (Figure 1c), clear showing its dispersion (right digital photograph in Scheme 1) as well as the small *D* in DLS (Figure S1a, agreeing to the size observed in SEM). In addition, the particle sizes of P@MOF increases as the degree of polymerization (DP) of P@MOF increases from 2P to 12P, as shown in Figure S1a and S1b, ascribing to the polymer grafted on the surface of the MOF core. Normally the hydrophobic nature[8] and/or strong interparticle interactions[15] of MOF nanoparticles are believed to be responsible for the strong aggregation tendency. As reflected by the 0^o contact angle in Figure S2, the NH_2-UiO-66 film showed super hydrophilicity. This result reveals that the aggregation of raw NH_2-UiO-66 is not assigned to the hydrophobicity nature but to the strong interparticle interactions. When grafted by hydrophilic PEG based brushes, the MOF particles were isolated from each other and thus such interaction was eliminated.

Figure 1d-i reflects the XPS spectra of MOF (NH_2-UiO-66), Br@MOF (0.5Br) and P@MOF (0.5Br-4P). From the wide scanning spectra we find that the XPS spectra of NH_2-UiO-66 (Figure 1d) includes the peaks of C1s (285 eV), O1s (530 eV), N1s (400 eV), Zr3p (334 eV) and Zr3d (184 eV), which is in good agreement with the chemical structure of NH_2-UiO-66.[16] A sharp new peak at 70 eV (corresponds to Br3d) shows up in the XPS spectrum of 0.5Br (Figure 1e), while the other peaks match to that of NH_2-UiO-66. This observation implies the successful functionalization of bromide to NH_2-UiO-66. The PEG shell in 0.5Br-4P makes the Zr signal undetectable in its XPS spectra, as shown in Figure 1f. The evolution of the C1s high-resolution scanning spectra for these samples further support the chemical structure evolution from NH_2-UiO-66 to Br@MOF and P@MOF. The C1s signal of NH_2-UiO-66 (Figure 1g) can be differentiated into 2 peaks at 285.1 eV and 288.8 eV, which are ascribed to the carbons on the benzoic ring (C1) and on the carboxyl (C2) of the ligand respectively. From Figure 1h we found that the bromide functionalization of NH_2-UiO-66 introduced a new peak at 286.8 eV which is assigned to the α-carbon of the bromoisobutyryl group (C3). The sharp, intensive peak for 0.5Br-4P (Figure 1i) at 286.5 eV is assigned to the carbon atoms of PEG based shell (C PEG). Again, the XPS measurements indicate the successful preparation of P@MOF.

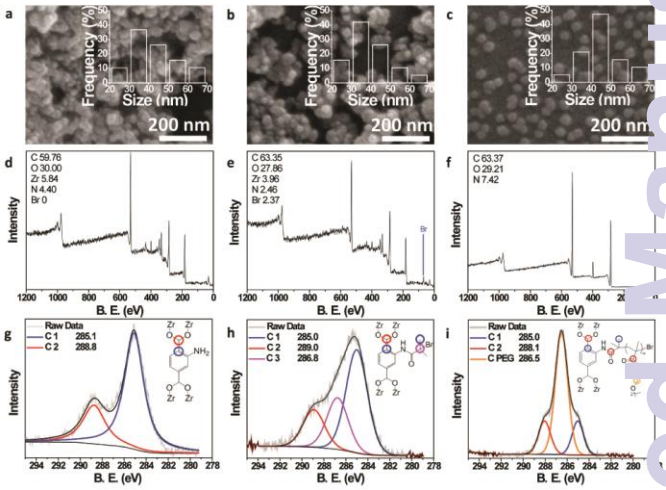

Figure 1 Illustration of the evolution of NH_2-UiO-66, Br-functionalized NH_2-UiO-66 (Br@MOF) and PEG grafted NH_2-UiO-66 (P@MOF). a-c) Typical SEM images for NH_2-UiO-66 (a), 0.5Br (b) and 0.5Br-4P (c). The corresponding size distributions are inserted. d-f) Wide-scan XPS spectra for NH_2-UiO-66 (d), 0.5Br (e) and 0.5Br-4P (f). The detected elements (at. %) are indicated at the corner. g-i) High-resolution C1s XPS spectra for NH_2-UiO-66 (g), 0.5Br (h) and 0.5Br-4P (i). The C1s peaks were differentiated and the carbon species assigned to the imitated peaks are circled with corresponding colour.

The crystallinity of raw MOF, Br@MOF and P@MOF were further investigated by XRD measurements (Figure S3). The observed XRD pattern of NH_2-UiO-66 (Figure S3a) is in good agreement with previous reports.[14] The bromo-functionalization did not change the crystal structure of raw MOF since the XRD pattern of 0.5Br is nearly identical to that of NH_2-UiO-66 (Figure S3b). Figure S3c represents the XRD spectra of 0.5Br-1P. The sharp peaks from the MOF core are partially overlapped with a wide peak from 10^o to 25^o which is ascribed to the amorphous PEG diffraction.[17] Higher DP of 0.5Br-4P results in the total concealment of the MOF peaks, as demonstrated in Figure S3d. XRD measurements here again indicate the successful synthesis and the preservation of pore structure for P@MOF. The degree of bromide functionalization in 0.5Br and the content of the polymer in P@MOF were measured by TGA in an air atmosphere (refer to Figure S4 and Table S1). It clearly shows that the polymer content increases with the feed quantity of the PEGMA.

From the digital image of 0.5Br-1P (Figure 2a) and its DLS curve in Figure S1a, we observe that at pH of 7, the 0.5Br-1P aqueous dispersion is slightly aggregated and the DLS peak size is smaller than NH_2-UiO-66 and 0.5Br but larger than the 0.5Br-4P because the polymer brush on 0.5Br-1P is too short to make it 100% dispersed. However, when the pH value was adjusted to 9, the 0.5Br-1P aqueous suspension transformed from emulsion-looking (Figure 2a and S4a) to a clear, transparent appearance (Figure 2a

and S4b). This means the 0.5Br-1P presents a pH-switchable dispersity in water. Correspondingly, its *D* reduced from 60-500 nm (aggregated) to 20-60 nm (well dispersed), implying a deaggregation process (Figure 2a). Once the pH was adjusted to 4, the transparent dispersion quickly turned cloudy (Figure S5c) and the particles precipitated within 3 minutes (Figure S5d). Moreover, all these transformations are reversible. This behaviour is ascribed to the pH stimulated formation and deformation of PEG brush-carboxyl group complex that could change the hydrophobicity of the PEG brush,[18–21] where the carboxylic groups comes from the partial uncoordinated ligands on the surface of MOF particles.[22–25] Interestingly, although the 0.5Br-2P and 0.5Br-4P water dispersions are clear at the pH of 7, it also turned cloudy when the pH was changed to 4. This is because their PEG brushes are long enough to make them well-dispersed at pH of 7, and less sensitive to the change of pH. The pH did not affect the dispersity of raw NH_2-UiO-66 particles since the effect of the carboxyl group protonate/deprotonate was too minor to influence the dispersity.

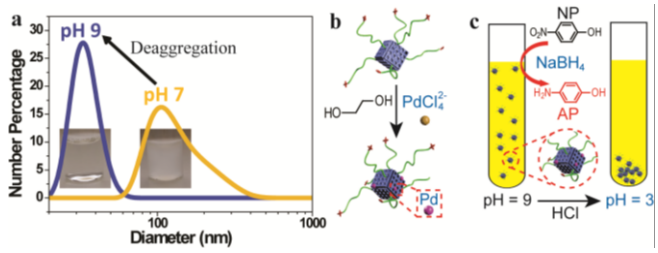

Figure 2 a) DLS curves indicating the deaggregation of 0.5Br-1P. b and c) Schematic representations for the preparation of Pd(0) loaded P@MOF (b) and the Pd(0)-P@MOF catalysed reduction reaction (c).

Table 1. Summary of the catalytic performance.

Sample	Pd (w.t. %)	TOF (h^{-1})[a]	2 hour TON[a]
Pd-0.5Br-1P	0.208	7.98	5.83
Pd-0.5Br-2P	0.215	5.94	5.18
Pd-0.5Br-4P	0.150	4.58	4.74
Pd-NH_2-UiO-66	0.175	2.26	3.43

[a]TOF and TON are calculated based on the total number of Pd(0) atoms.

As discussed earlier, compared with the aggregated MOF particles, the better dispersity of P@MOF is expected to reduce the mass transfer resistance between inner porous space of MOF and the bulk phase. Herein, we compared the performance of aggregated MOF and well-dispersed P@MOF as the catalyst carrier to demonstrate the benefit of improved dispersity. In addition to higher catalytic activity, 0.5Br-1P based catalyst can be conveniently recycled similar to the common heterogeneous catalyst by acidifying the solution due to the pH-switchable feature of its dispersity. As shown in Figure 2b, Pd(0) was loaded onto the P@MOFs by reducing Pd(II) via a well-established ethylene glycol reducing method.[26,27] The loading ratio (w.t.) of Pd(0) are 0.208%, 0.215%, 0.150% and 0.175% for Pd-0.5Br-1P, Pd-0.5Br-2P, Pd-0.5Br-4P and Pd-NH_2-UiO-66, respectively, as measured by ICP-OES (Table 1). Pd(0) catalysed reduction of 4-nitrophenol (NP) to 4-aminophenol (AP) by sodium borohydride ($NaBH_4$) was used as the probe reaction to study the catalytic performance of Pd(0) loaded P@MOFs (Figure 2c).[28–30] The dynamics were investigated by UV-vis spectrophotometry since the NP has absorption at 405 nm while AP has no absorption at the same position (but at 295 nm).[28–30] As illustrated in Figure 3a, after the introduction of the Pd-0.5Br-1P, the absorption at 405 nm decreases while the absorption at 295 nm increases gradually, indicating the reduction of NP and the generation of AP. The pH of this solution is 9 due to the partial hydrolysis of the $NaBH_4$, hence the Pd(0)-loaded P@MOFs were well dispersed in solution, while the Pd-NH_2-UiO-66 was still aggregated. As a result, the activities of the Pd(0)-loaded P@MOFs are higher than that of Pd-NH_2-UiO-66 because of their lower mass transfer resistance, as deduced from the conversion kinetics in Figure 3b, also from the turnover frequency (TOF) and turnover number (TON) values shown in Table 1. However, the higher Br of the P@MOF results in lower activities of Pd(0)-loaded P@MOFs (Figure 3b, Table 1) attributing to their relatively thicker PEG shell which reduce the diffusion of reactant and product. 0.5Br-1P without Pd(0) was used as the control and shows negligible activity (Figure 3b). Pd-0.5Br-1P can be efficiently recycled by adjusting the pH value to 3 (Figure 2c) and its recyclability was studied. As seen from the conversion kinetics of Pd-0.5Br-1P for different cycles in Figure 3c, the overall activity dropped from Cycle 1 to Cycle 3. To further study the reasons for this decayed performance, we measured the material recyclability and calculated the TOF value (reflects the normalized Pd(0) activity) for each cycle.

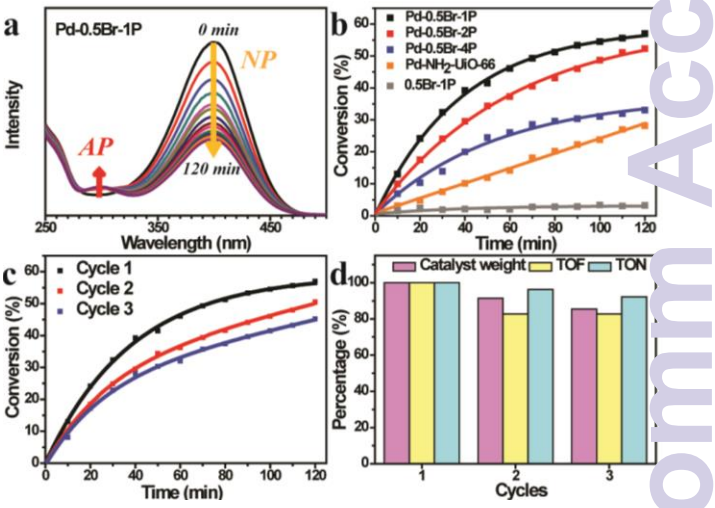

Figure 3 Catalytic performance of Pd(0) loaded P@MOFs. a) UV-vis absorption evolution spectra as hydrogenation time elapsing. Time between curves is 10 minutes. b) Conversion versus time plots of indicated catalyst. c) Conversion versus time plots of Pd-0.5Br-1P for 3 cycles. d) Column chart showing the recyclability of Pd-0.5Br-1P. The TON is based on the conversion at the 120th minute.

As presented in Figure 3d, the mass of Pd-0.5Br-1P gradually decreased (100%, 91.5% and 85.4% for Cycle 1, 2 and 3 respectively) for each cycle because of the unavoidable loss of materials during the recycle, similar to the common heterogeneous catalysts.[31] From the TOF for each cycle we can see that the Pd(0) activity firstly

dropped 17 % after Cycle 1 and remained nearly constant for Cycle 2 and Cycle 3. Therefore, the decay of the activity from Cycle 1 to Cycle 2 is attributed to both the material loss and decreased Pd(0) activity, whereas the decay of the activity from Cycle 2 to Cycle 3 is ascribed to the materials loss only. Additionally, the 2 hour TON value dropped *ca.* 4% after each cycle. Despite the small activity decay, all these results still indicate the good overall recyclability of Pd-0.5Br-1P which is similar to the ordinary MOF supported heterogeneous catslyst.[32–34] As seen, the Pd-0.5Br-1P integrates the advantages of both homogeneous (higher activity) and heterogeneous (better recyclability) catalyst. Furthermore, based on such a special integrated feature, *i.e.* dispersible solvent, highly porous and core-shell configuration, we believe the P@MOF would potentially show wide applications in the fields including drug delivery, small molecule adsorption/separation, printable devices, water treatment and fuel cells *etc*.

Conclusions

In summary, a core-shell material P@MOF has been prepared via a two-step procedure at ambient conditions. The P@MOF composite nanoparticles can be well-dispersed in water, and for the particles with short grafted chains, the dispersity is pH-switchable. Pd(0) was successfully loaded onto P@MOF particles. The Pd-0.5Br-1P catalyst integrates both the benefits of homogeneous (higher activity) and heterogeneous (better recyclability) catalysts.

The authors acknowledge the Australian Research Council under the Future Fellowship (FT110100411, G.G.Q.).

Notes and references

1 H.-C. 'Joe' Zhou and S. Kitagawa, *Chem. Soc. Rev.*, 2014, **43**, 5415–5418.
2 A. Schneemann, V. Bon, I. Schwedler, I. Senkovska, S. Kaskel and R. A. Fischer, *Chem. Soc. Rev.*, 2014, **43**, 6062–6096.
3 J. D. Evans, C. J. Sumby and C. J. Doonan, *Chem. Soc. Rev.*, 2014, **43**, 5933–5951.
4 J. Liu, L. Chen, H. Cui, J. Zhang, L. Zhang and C.-Y. Su, *Chem. Soc. Rev.*, 2014, 6011–6061.
5 V. Stavila, A. A. Talin and M. D. Allendorf, *Chem. Soc. Rev.*, 2014, **43**, 5994–6010.
6 B. Van de Voorde, B. Bueken, J. Denayer and D. De Vos, *Chem. Soc. Rev.*, 2014, **43**, 5766–5788.
7 P. Horcajada, T. Chalati, C. Serre, B. Gillet, C. Sebrie, T. Baati, J. F. Eubank, D. Heurtaux, P. Clayette, C. Kreuz, J.-S. Chang, Y. K. Hwang, V. Marsaud, P.-N. Bories, L. Cynober, S. Gil, G. Férey, P. Couvreur and R. Gref, *Nat. Mater.*, 2010, **9**, 172–178.
8 Q.-L. Zhu and Q. Xu, *Chem. Soc. Rev.*, 2014, **43**, 5648–5512.
9 J. Huo, M. Marcello, A. Garai and D. Bradshaw, *Adv. Mater.*, 2013, **25**, 2717–2722.
10 D. Liu, R. C. Huxford and W. Lin, *Angew. Chemie - Int. Ed.*, 2011, **50**, 3696–3700.
11 W. Zhang, Y. Hu, J. Ge, H. Jiang and S. Yu, *J. Am. Chem. Soc.*, 2014, **136**, 16978–16981.
12 A. Halim, Q. Fu, Q. Yong, P. Gurr, S. E. Kentish and G. G. Qiao, *J. Mater. Chem. A*, 2014, **2**, 4999–5009.
13 D. Mertz, C. J. Ochs, Z. Zhu, L. Lee, S. N. Guntari, G. K. Such T. K. Goh, L. A. Connal, A. Blencowe, G. G. Qiao and F. Caruso, *Chem. Commun.*, 2011, **47**, 12601–12603.
14 A. Schaate, P. Roy, A. Godt, J. Lippke, F. Waltz, M. Wiebcke and P. Behrens, *Chem. - A Eur. J.*, 2011, **17**, 6643–6651.
15 D. Zhao, S. Tan, D. Yuan, W. Lu, Y. H. Rezenom, H. Jiang, L. Q. Wang and H. C. Zhou, *Adv. Mater.*, 2011, **23**, 90–93.
16 J. Long, S. Wang, Z. Ding, S. Wang, Y. Zhou, L. Huang and X Wang, *Chem. Commun.*, 2012, **48**, 11656–11658.
17 Q. Fu, A. Halim, J. Kim, J. Scofield, P. Gurr, S. E. Kentish and G. G. Qiao, *J. Mater. Chem. A*, 2013, **1**, 13769–13778.
18 X. Laloyaux, B. Mathy, B. Nysten and A. M. Jonas, *Macromolecules*, 2010, **43**, 7744–7751.
19 O. E. Philippova, N. S. Karibyants and S. G. Starodubtzev, *Macromolecules*, 1994, **27**, 2398–2401.
20 Y. Stetsyshyn, K. Fornal, J. Raczkowska, J. Zemla, A. Kostruba, H. Ohar, M. Ohar, V. Donchak, K. Harhay, K. Awsiuk, J. Rysz, A. Bernasik and A. Budkowski, *J. Colloid Interface Sci.*, 2013, **411**, 247–256.
21 V. V Khutoryanskiy, A. V Dubolazov, Z. S. Nurkeeva and G. a Mun, *Langmuir*, 2004, **20**, 3785–3790.
22 L. Wen, Z. Lu, J. Lin, Z. Tian, H. Zhu and Q. Meng, *Cryst. Growth Des.*, 2007, **7**, 93–99.
23 A. Vimont, J. M. Goupil, J. C. Lavalley, M. Daturi, S. Surblé, C. Serre, F. Millange, G. Férey and N. Audebrand, *J. Am. Chem. Soc.*, 2006, **128**, 3218–3227.
24 H. He, F. Dai, A. Xie, X. Tong and D. Sun, *CrystEngComm*, 2008, **10**, 1429–1435.
25 F. A. A. Paz and J. Klinowski, *Inorg. Chem.*, 2004, **43**, 3882–3893.
26 S. Jiang, Y. Ma, G. Jian, H. Tao, X. Wang, Y. Fan, Y. Lu, Z. Hu and Y. Chen, *Adv. Mater.*, 2009, **21**, 4953–4956.
27 Y. Xiong, J. M. Mclellan, J. Chen, Y. Yin, Z. Li and Y. Xia, *J. Am. Chem. Soc.*, 2005, **127**, 17118–17127.
28 S. H. Wibowo, A. Sulistio, E. H. H. Wong, A. Blencowe and G. G. Qiao, *Adv. Funct. Mater.*, 2015, DOI: 10.1002/adfm.201404091.
29 Y. Lu, Y. Mei, M. Drechsler and M. Ballauff, *Angew. Chemie - Int. Ed.*, 2006, **45**, 813–816.
30 G. Marcelo, A. Muñoz-Bonilla and M. Fernández-García, *J. Phys. Chem. C*, 2012, **116**, 24717–24725.
31 J. A. Bennett, I. P. Mikheenko, K. Deplanche, I. J. Shannon, J. Wood and L. E. Macaskie, *Appl. Catal. B Environ.*, 2013, **140-141**, 700–707.
32 Z. Xu, L. Han, G. Zhuang, J. Bai and D. Sun, *Inorg. Chem.*, 2015, **54**, 4737–4743.
33 K. M. Choi, K. Na, G. A. Somorjai and O. M. Yaghi, *J. Am. Chem. Soc.*, 2015, **137**, 7810–7816.
34 A. Henschel, K. Gedrich, R. Kraehnert and S. Kaskel, *Chem. Commun.*, 2008, 4192–4194.